Supplementary Text. Extended Description of the Ras model and Supplementary Methods

Extended Description of the Ras model

Reactions included in the Ras model

Our model of the Ras signaling network focuses on the core processes that regulate Ras signals (fig. S1). These reactions include:

i) Intrinsic GTPase activity of the Ras protein
ii) Spontaneous dissociation of GTP from GTP bound Ras proteins
iii) Spontaneous dissociation of GDP from GDP bound Ras proteins
iv) Spontaneous association of GTP to nucleotide-free Ras proteins
v) Spontaneous association of GDP to nucleotide-free Ras proteins
vi) Association of Ras to an Effector protein to form a Ras-Effector complex
vii) The dissociation of Ras-Effector complexes into Ras and Effector
viii) Intrinsic GTPase activity of the Ras protein within a Ras-Effector complex
ix) GAP mediated GTP hydrolysis
x) GEF mediated exchange of GDP for GTP
xi) GEF mediated exchange of GTP for GDP

Model Equations

Each of the eleven reactions described above can be well described mathematically as a biochemical reaction. Moreover, both the wild-type and mutant proteins can be described by the same equations, but with different parameters to account for measured differences between wild-type and mutant proteins.

For each of the reactions below, terms beginning with a lower case "k" are kinetic rate constants, terms beginning with a "V" are enzymatic V_{max} terms, terms beginning with a capital "K" are Michaelis-constants (K_m), and cellular abundances are indicated in square brackets ("[]") with the species of interest indicated between the brackets.

i) Intrinsic GTPase activity of the Ras protein

R1-WT: $k_{GTPase,WT}$ [RasWT,GTP]
R1-MUT: $k_{GTPase,MUT}$ [RasMUT,GTP]

Where [RasWT,GTP] indicates wild-type Ras bound to GTP but not to effector, and where [RasMUT,GTP] indicates mutant Ras bound to GTP but not to effector.

The intrinsic GTPase activity of the Ras protein can be specified with first order mass action kinetics. Distinct parameter values are used for wild-type and mutant proteins, accounting for the much slower rate of spontaneous GTPase activity that has been noted for many of the common oncogenic Ras mutants.

Note: for this and for many of the following reactions, H_20, GTP, GDP, and phosphate are not explicitly included. It is here assumed (or approximated) that the cell maintains constant levels of these entities over time. The reaction parameters may be thought of as effective parameters that account for this assumption.

ii) Spontaneous dissociation of GTP from GTP bound Ras proteins

R2-WT: $k_{d,GTP,WT}$ [RasWT,GTP]
R2-MUT: $k_{d,GTP,MUT}$ [RasMUT,GTP]

Spontaneous dissociation of GTP from wild-type and mutant Ras is modeled with first order mass action kinetics.

iii) Spontaneous dissociation of GDP from GDP bound Ras proteins

R3-WT: $k_{d,GDP,WT}$ [RasWT,GDP]
R3-MUT: $k_{d,GDP,MUT}$ [RasMUT,GDP]

Where [RasWT,GDP] indicates wild-type Ras bound to GDP but not to effector, and where [RasMUT,GDP] indicates mutant Ras bound to GTP but not to effector.

Spontaneous dissociation of GTP from wild-type and mutant Ras is modeled with first order mass action kinetics.

iv) Spontaneous association of GTP to nucleotide-free Ras proteins

R4-WT: $k_{a,GTP,WT}$ [RasWT] [GTP]
R4-MUT: $k_{a,GTP,MUT}$ [RasMUT] [GTP]

Where [RasWT] indicates wild-type Ras bound not bound to any nucleotide or to effector, [RasMUT] indicates mutant Ras not bound to any nucleotide or to effector, and [GTP] indicates cellular GTP.

The association of GTP with Ras can be modeled with second order mass action kinetics.

v) Spontaneous association of GDP to nucleotide-free Ras proteins

R5-WT: $k_{a,GDP,WT}$ [RasWT] [GDP]
R5-MUT: $k_{a,GDP,MUT}$ [RasMUT] [GDP]

The association of GDP with Ras can be modeled with an equation equivalent to second order mass action kinetics, as was done for GTP association, above.

vi) Association of Ras to an Effector protein to form a Ras-Effector complex

R6-WT: $k_{a,Eff,WT}$ [RasWT,GTP] [Effector]
R6-MUT: $k_{a,Eff,MUT}$ [RasMUT,GTP] [Effector]

Where [Effector] indicates proteins that specifically bind to RasGTP but are not yet bound to Ras.

The association of Ras with Effector proteins can be modeled with second order mass action kinetics.

vii) The dissociation of Ras-Effector complexes into Ras and Effector

R7-WT: $k_{d,Eff,WT}$ [RasWT,GTP-Effector]
R7-MUT: $k_{d,Eff,MUT}$ [RasMUT,GTP-Effector]

Where [RasWT,GTP-Effector] indicates a wild-type Ras protein that is bound to an Effector protein, and where [RasMUT,GTP-Effector] indicates a mutant Ras protein that is bound to an Effector protein.

The dissociation of Ras-Effector complex into the individual Ras and Effector proteins can be modeled with first order mass action kinetics.

viii) Intrinsic GTPase activity of the Ras protein within a Ras-Effector complex

R8-WT: $k_{GTPase,WT}$ [RasWT,GTP-Effector]
R8-MUT: $k_{GTPase,MUT}$ [RasMUT,GTP-Effector]

The intrinsic GTPase activity of a Ras protein bound to an Effector protein is modeled with first order mass action kinetics. Here, we assume that the rate constants for these reactions is equivalent to the rate constant for RasGTP not bound to an effector as there is not, to the best of our knowledge, sufficient data to warrant modeling this with a different reaction rate constant.

ix) GAP-mediated GTP hydrolysis

R9-WT: $V_{max,WT,GAP}$ [RasWT,GTP]/(GAP-DEN)
R9-MUT: $V_{max,MUT,GAP}$ [RasMUT,GTP]/(GAP--DEN)

Where GAP-DEN is: $1 + [RasWT,GTP]/K_{m,WT} + [RasMUT,GTP]/K_{m,MUT}$
Where $V_{max,WT,GAP} = k_{cat,WT}$ [GAPactive]
And where $V_{max,MUT,GAP} = k_{cat,MUT}$ [GAPactive]
And [GAPactive] indicates the quantity of enzymatically active and appropriately localized GAP (it does not indicate total cellular GAP) .

GAP-mediated GTP hydrolysis is here modeled with competitive, irreversible, Michaelis-Menten kinetics. This allows experimentally determined k_{cat} and K_m values to be utilized. Additionally, multi-step enzymatic reactions can simplify to a Michaelis-Menten form. Lastly, we will focus on steady-state solutions so we will not be affected by initial phase transient

artifacts. At steady-state, the pseudo-steady-state hypothesis that is used to derive the Michaelis-Menten equation necessarily holds. We utilize competitive Michaelis-Menten kinetics, as the enzymatic site of a Ras GAP protein (like NF1) may bind to either wild-type or Mutant Ras protein.

x) GEF mediated exchange of GDP for GTP

R10-WT: $V_{max,WT,GEF,GDP}$ ([RasWT,GDP]/$K_{m,WT,GDP}$)/(GEF-DEN)
R10-MUT: $V_{max,MUT,GEF,GDP}$ ([RasMUT,GDP]/$K_{m,MUT,GDP}$)/(GEF-DEN)

Where GEF-DEN is:

$1 + [RasWT,GDP]/K_{m,WT,GDP} + [RasWT,GTP]/K_{m,WT,GTP} + [RasMUT,GDP]/K_{m,MUT,GDP} + [RasMUT,GTP]/K_{m,MUT,GTP}$

GEF-mediated GTP hydrolysis is here modeled with competitive, reversible, Michaelis-Menten kinetics. This allows experimentally determined k_{cat} and K_m values to be utilized. Additionally, multi-step enzymatic reactions can similarly simplify to a Michaelis-Menten form, so this approach can be more general when every step of a multi-step reaction is not known. Lastly, we will be focusing on steady-state solutions, so we will not be affected by spurious transients and the pseudo-steady-state hypothesis that is used to derive the Michaelis-Menten equation holds at steady-state. We utilize competitive Michaelis-Menten kinetics, as the enzymatic site of a Ras GEF protein (like SOS1 or SOS2) may bind to either wild-type or Mutant Ras protein. We use reversible Michaelis-Menten kinetics because Ras family GEFs appear capable of catalyzing nucleotide exchange on both GTP bound and GDP bound Ras. For example, many experiments study nucleotide exchange on GTP-loaded GTPases in addition to (or in place of) GDP-loaded GTPases (REFs).

xi) GEF mediated exchange of GTP for GDP

R11-WT: $V_{max,WT,GEF,GTP}$ ([RasWT,GTP]/$K_{m,WT,GTP}$)/(GEF-DEN)
R11-MUT: $V_{max,MUT,GEF,GTP}$ ([RasMUT,GTP]/$K_{m,MUT,GTP}$)/(GEF -DEN)

Where GEF-DEN is:

$1 + [RasWT,GDP]/K_{m,WT,GDP} + [RasWT,GTP]/K_{m,WT,GTP} + [RasMUT,GDP]/K_{m,MUT,GDP} + [RasMUT,GTP]/K_{m,MUT,GTP}$

Full model

Within a cell, these reactions are all be occurring simultaneously to influence the cellular level of Ras in its different states. Mathematically, we combine these individual reactions into a system of ordinary differential equations to describe these collective processes. We need one equation for each of the nine species that we consider (RasWT,GTP; RasWT; RasWT,GDP; RasWT,GTP-Effector; RasMut,GTP; RasMut; RasMut,GDP; RasMut,GTP-Effector; Effector). We consider levels of GEF and GAP to be much smaller than levels of Ras and Effector, and they are effectively considered within the Michaelis-Menten equations above.

dRasWT,GTP/dt = – (R1-WT) – (R2-WT) + (R4-WT) – (R6-WT) + (R7-WT) – (R9-WT) + (R10-WT) – (R11-WT)

dRasWT/dt = + (R2-WT) + (R3-WT) – (R4-WT) – (R5-WT)

dRasWT,GDP/dt = + (R1-WT) – (R3-WT) + (R5-WT) + (R8-WT) + (R9-WT) – (R10-WT) + (R11-WT)

dRasWT,GTP-Effector/dt = + (R6-WT) – (R7-WT) – (R8-WT)

dRasMut,GTP/dt = – (R1-MUT) – (R2-MUT) + (R4-MUT) – (R6-MUT) + (R7-MUT) – (R9-MUT) + (R10-MUT) – (R11-MUT)

dRasMut/dt = + (R2-MUT) + (R3-MUT) – (R4-MUT) - (R5-MUT)

dRasMut,GDP/dt = + (R1-MUT) – (R3-MUT) + (R5-MUT) + (R8-MUT) + (R9-MUT) – (R10-MUT) + (R11-MUT)

dRasMut,GTP-Effector/dt = + (R6-MUT) – (R7-MUT) – (R8-MUT)

dEffector/dt = – (R6-WT) – (R6-MUT) + (R7-WT) + (R7-MUT) + (R8-WT)
+ (R8-MUT)

Parameters of the Model

Molecular abundances

We model two pools of Ras proteins, one of wild-type Ras and one of mutant Ras. We group wild-type HRAS, NRAS, and KRAS into a single pool of wild-type Ras because the biochemical properties of these three proteins are quite similar (*39, 40*). However, one could easily extend the model to include wild-type forms of HRAS, NRAS, and KRAS using the same equations as above and utilizing the slightly different parameter values for each. We similarly group all Ras effectors into a single pool of Ras effectors, all active Ras GAPs into a single pool of active Ras GAPs, and all active Ras GEFs into a single pool of Ras GEFs. We estimate total, cellular, Ras at 0.4 μM, total, cellular, Ras Effectors at μM GTP at 180 μM, GDP at 18 μM. Estimated abundances of total, active, cellular Ras GEFs and total, active, cellular Ras GAPs are effectively included in estimated V_{max} terms, below.

Wild-type Ras Parameters

For each of the wild-type Ras parameters indicated above, we have previously identified experimental measurements for each parameter (*15*). These are the same values as used in our original Ras manuscript and that have been utilized in our subsequent studies. For interactions between Ras and effectors, we used the interactions between Ras and Raf to define this class of reactions. For interactions between Ras and Ras GAPs, we used data from the interaction between Ras and NF1 to be representative of all interactions between Ras and basally active Ras GAPs. For interactions between Ras and Ras GEFs, we used data from the interaction between Ras and RasGRF1 to be representative of all interactions between Ras and basally active Ras GEFs, choosing RasGRF1 as our representative GEF because this specific set of reactions has been very well quantified at the level of detail required for our model (*39*).

$\mathbf{k_{GTPase,WT}}$	$= 3.5 \times 10^{-4}$/s (*38*)
$\mathbf{k_{d,GTP,WT}}$	$= 2.5 \times 10^{-4}$/s (*38*)
$\mathbf{k_{d,GDP,WT}}$	$= 1.1 \times 10^{-4}$/s (*38*)
$\mathbf{k_{a,GTP,WT}}$	$= 2.2 \times 10^{6}$/Ms (*39*)
$\mathbf{k_{a,GDP,WT}}$	$= 2.3 \times 10^{6}$/Ms (*39*)
$\mathbf{k_{a,Eff,WT}}$	$= 4.5 \times 10^{7}$/Ms (*43*)
$\mathbf{k_{d,Eff,WT}}$	$= 3.6 \times 10^{0}$/s (*15, 44*)
$\mathbf{V_{max,WT,GAP}}$	$= 3.24 \times 10^{-10}$ M/s (*15, 40*)
$\mathbf{K_{m,WT}}$	$= 0.23 \times 10^{-6}$ M (*40*)
$\mathbf{V_{max,WT,GEF,GDP}}$	$= 7.8 \times 10^{-10}$ M/s (*15, 39*)
$\mathbf{K_{m,WT,GDP}}$	$= 3.86 \times 10^{-4}$ M (*39*)
$\mathbf{V_{max,WT,GEF,GTP}}$	$= 1.4404 \times 10^{-10}$ M/s (*15, 39*)
$\mathbf{K_{m,WT,GTP}}$	$= 3.0 \times 10^{-4}$ M (*39*)

Mutant Ras parameters

Many of these exact same reactions have also been quantified for mutant proteins. To compare parameters between studies, we have taken the approach of applying the change in the parameter to the wild-type parameter value in the same study and using this factor to scale the value we had used in our wild-type protein parameterization. We refer to this ratio of the mutant parameter value to the wild-type parameter value from a study as α. We then calculate the mutant parameter value by multiplying the α value for the specific parameter and mutant to the corresponding parameter value for wild-type Ras. When no data is available, we assume no change and use an of α value 1 so that we may determine whether the known differences are sufficient to explain observed differences between the Ras mutants.

	G12V	**G12D**	**G13D**
$\mathbf{k_{GTPase,MUT}}$	0.15 (*35*)	0.40 (*35*)	0.40 (*35*)
$\mathbf{k_{d,GTP,MUT}}$	0.80 (*35*)	5.00 (*35*)	3.63 (*18*)
$\mathbf{k_{d,GDP,MUT}}$	0.31 (*35*)	0.48 (*35*)	3.63 (*18*)
$\mathbf{k_{a,GTP,MUT}}$	4.14 (*35*)	3.43 (*35*)	1
$\mathbf{k_{a,GDP,MUT}}$	2.27 (*35*)	1.37 (*35*)	1
$\mathbf{k_{a,Eff,MUT}}$	1	1	1
$\mathbf{k_{d,Eff,MUT}}$	0.44 (*36*)	1	1
$\mathbf{V_{max,MUT,GAP}}$	0 (*35*)	0 (*35*)	0 (*35*)
$\mathbf{K_{m,MUT}}$	1	1	100 (*17*)
$\mathbf{V_{max,MUT,GEF,GDP}}$	1	1	1
$\mathbf{K_{m,MUT,GDP}}$	1	1	1
$\mathbf{K_{m,MUT,GTP}}$	1	1	1

For GTP hydrolysis defect of G13D, we used the save factor as for the G12D mutant. This was because we could not find a specific value for the G13D mutant at the time this project was initiated, and this choice allowed us to include the defect known to be present. It also allowed us

to focus on known quantitative differences between G13D, G12D, and G12V. The original Ras model manuscript provides a much longer discussion of modeling mutants, including discussions of how the $k_{cat,MUT,GEF,GDP}$ that feeds into the $V_{max,MUT,GEF,GDP}$ term must be calculated (*15*).

Membrane Localization Adjustments

Ras is membrane localized. Effector proteins are generally cytosolic, but can be recruited to the membrane through binding to Ras. GEFs and GAPs are also generally cytosolic, but they are recruited to the membrane where they act upon Ras. Although many of these reactions will occur on a 2-dimensional membrane, most of the parameter values have been measured in 3-dimensional solution. When we originally developed our model, we utilized the previously described approach of scaling 3-dimensional K_m values by a scaling factor of 1/D, where D has the value of 250. Subsequent work further suggests this approach and this value works well for problems in Ras biology (*31*).

Supplementary Methods

AKT phosphorylation

The pAKT antibodies were validated by starving WT SW48 cells in RPMI pen/strp media for 12 hours, cells were stimulated with EGF (50ng/ml) for 5 minutes. Whole cell lysates were prepared and resolved on 12% polyacrylamide gel. Gels were transferred to PDF membrane, and probed with anti-phospho-T308 AKT1 rabbit antibody (AB13038, Cell Signaling Technology), anti-phospho-S473 AKT1 rabbit monoclonal antibody (AB4060, Cell Signaling Technology) and anti-pan AKT mouse monoclonal antibody (AB2920, Cell Signaling Technology) in 3% Bovine Serum Albumin solution. Cell lines indicated were either treated with vehicle-control (Ctrl) or 20ug/ml of Cetuximab for 48 hours. Whole cell lysates were prepared and analyzed by western blot analysis as previously described.

Bioluminescence Resonance Energy Transfer (BRET) Assay

HEK-293T cells were grown in DMEM 10% FBS without antibiotic. Cells were seeded at $5x10^3$ cells per well in a 96 well white opaque Perkin Elmer microplate. 24 hours post-seeding, cells were co-transfected with a constant concentration 0.1 μg of NF1-NanoLuc pcDNA expression plasmid and increasing concentrations RAS-EGFP pcDNA expression plasmid (0, 0.05, 0.1, 0.2, 0.4, 0.6, 0.8 and 1.2 μg) with 0.25ul of Lipofectamine 2000 per well following manufacturers protocol (Thermo Fisher). 24 hours later, media was aspirated from each well and 25μl of Nano-Glo Live Cell Reagent was added to each well per manufacturer's protocol (Promega). Plates were placed on orbital shaker for 1 minute at 300 RPM. Following incubation, the plate was read on the Tecan Infinite M200 Pro with LumiColor Dual Setting with an integration time of 1000ms. BRET ratio was calculated from the dual emission readings: . BRET ratio was plotted as a function of the RAS-GFP/NF1-NanoLuc plasmid ratio. BRET assays were repeated five times, each with 8 biological replicates.

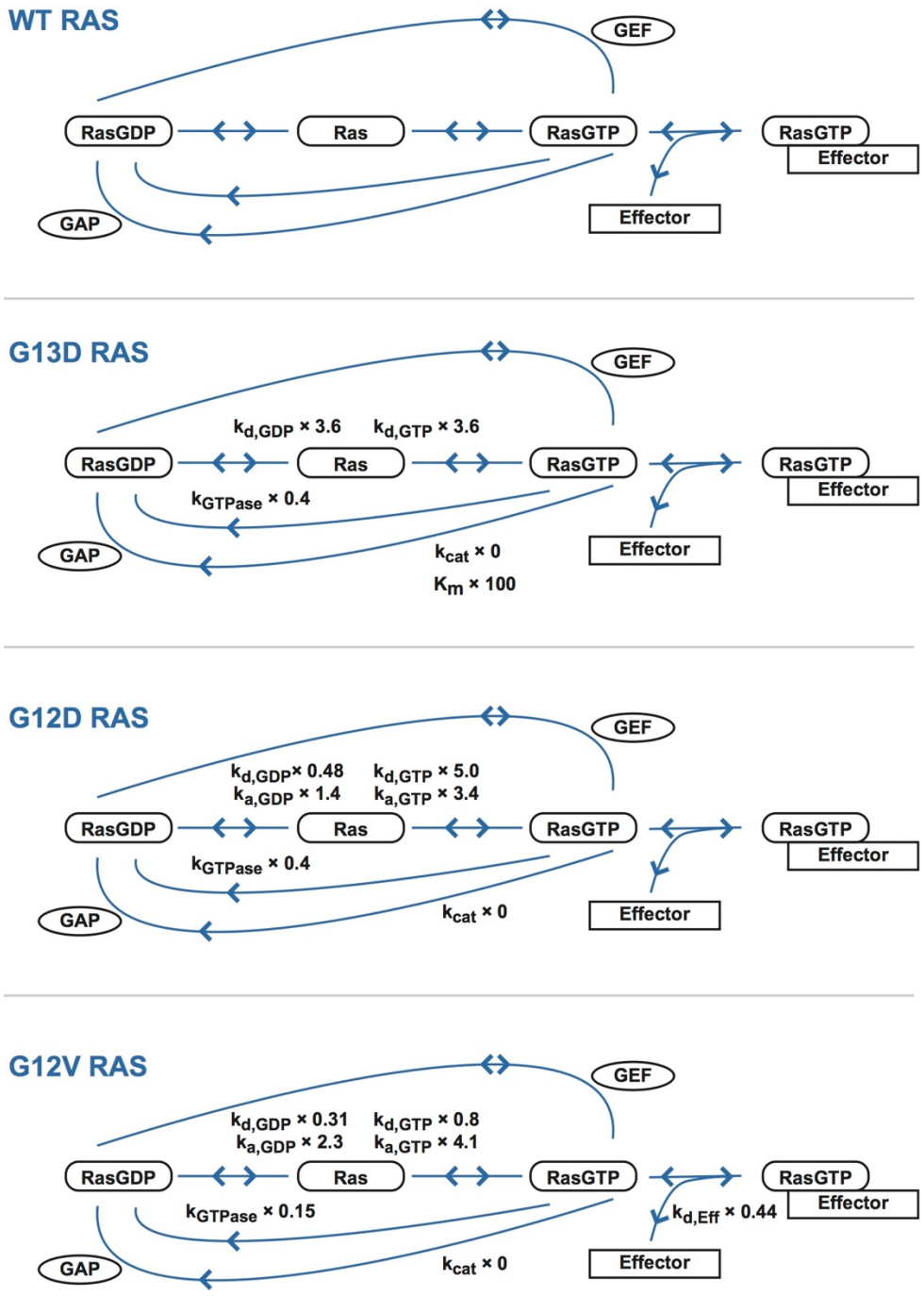

Fig. S1. Schematic of the reactions of the Ras model. The Ras model focuses on the processes that influence the Ras signaling state. The model includes interactions between Ras with GEFs, GAPs, and Effectors as well as slower nucleotide exchange and GTP hydrolysis reactions. For clarity, GTP, GDP, and phosphate ion are not indicated. For oncogenic mutants G13D, G12D, and G12V, the network is organized identically, but the specific parameters of the reaction rates can differ from the wild-type value. Parameters that differ between each mutant and wild-type are indicated; the value shown is the factor by which the indicated parameter of the mutant differs from the wild-type value.

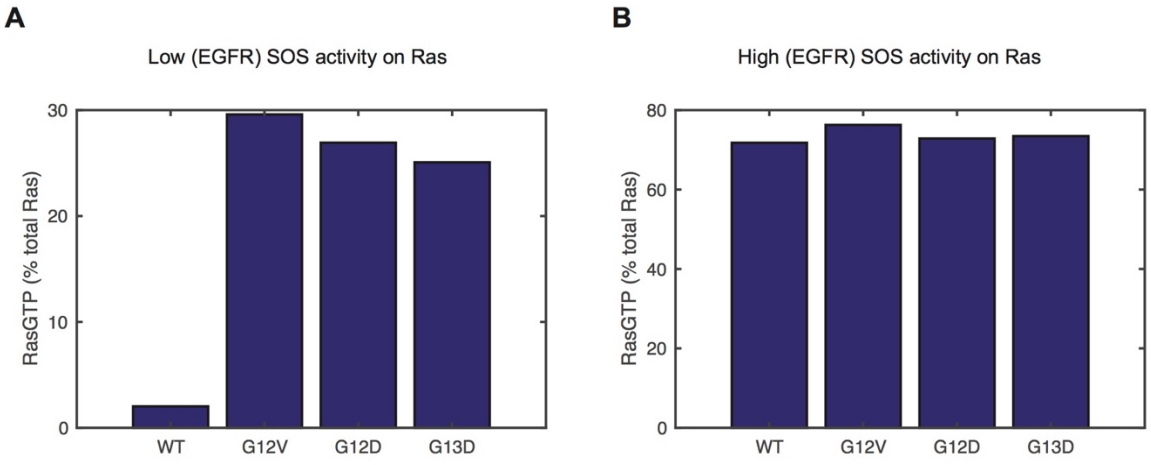

Fig. S2. Available parameters for the Ras G13D mutant are sufficient to account for its constitutive activation. (**A**) Model simulations were used to find the amount of RasGTP at basal conditions with a low abundance of active Ras GEFs (SOS1/2). Four different conditions were considered: when all Ras is wild-type (WT), or when one modeled allele is Ras G12V, G12D, or G13D. (**B**) Model simulations were used to find the amount of RasGTP at conditions with a high abundance of active Ras GEFs (SOS1/2), such as would occur when EGFR is activated, for the same four modeled genotypes as in A.

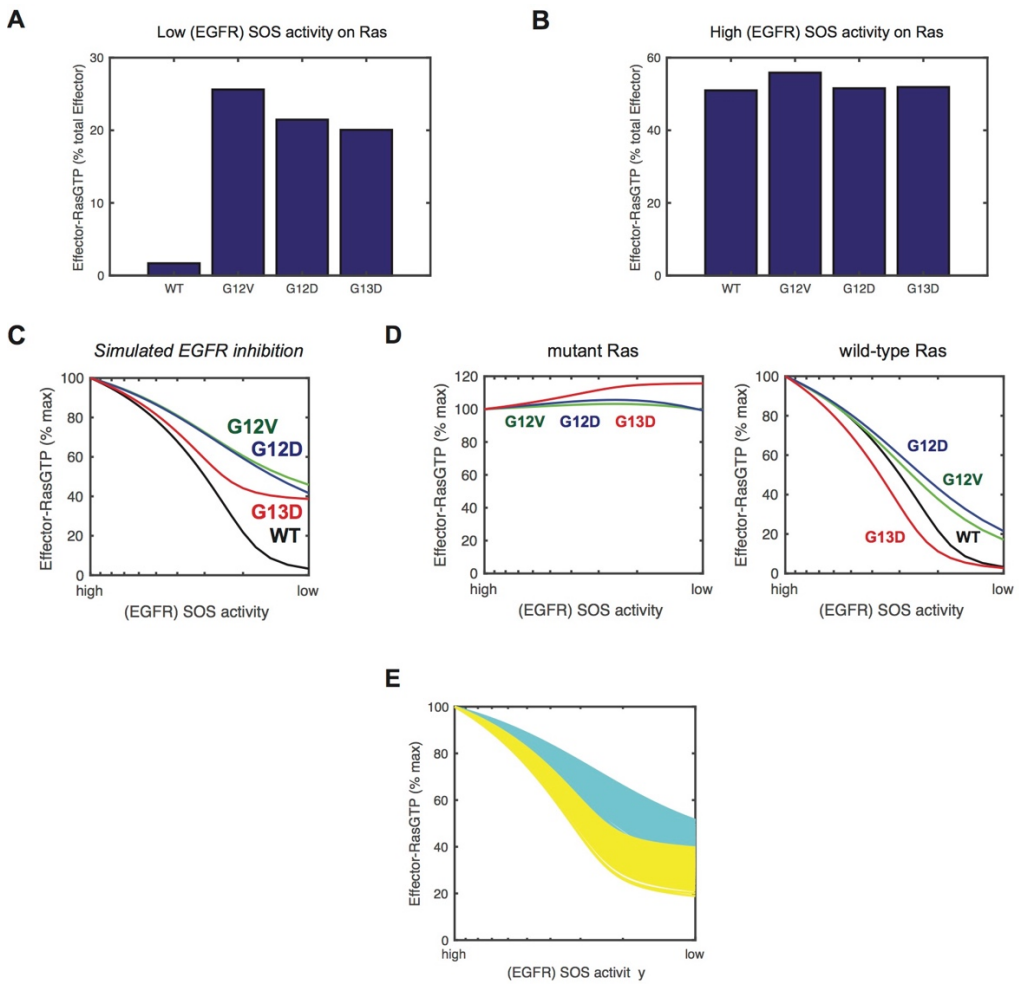

Fig. S3. Ras model predictions when level of RasGTP-Effector complex is used as a readout of signal strength instead of RasGTP. (**A**) Model simulations were used to find the amount of RasGTP-Effector complex at basal conditions with low GEF (SOS) mediated activation of Ras. Four different conditions were modeled: when all Ras is wild-type (WT), or when one Ras allele is G12V, G12D, or G13D. Corresponds to Fig. S2A. (**B**) Model simulations were used to find the amount of RasGTP-Effector complex at conditions of high GEF (SOS1/2) mediated activation of Ras, such as occurs when EGFR is activated, for the same four modeled genotypes as in A. Corresponds to Fig. S2B. (**C**) Simulated anti-EGFR dose response from the computational Ras model. Corresponds to Fig. 1B, but uses Ras-GTP Effector complex as the readout of signal strength. (**D**) Simulated anti-EGFR dose response for the Ras model, further subdivided to reveal the change in active, GTP-bound mutant Ras (left) and the change in active, GTP-bound wild-type Ras (right), each as a fraction of total H/N/KRAS within each modeled genotype. Corresponds to Fig. 2A, but uses Ras-GTP Effector complex as the readout of signal strength. (**E**) Simulated dose responses for 648 computational hybrid Ras mutants that were created by shuffling the parameters of KRAS G13D, G12D, and G12V. Each dose response is color coded on the basis of whether the hybrid had the Ras/NF1 K_m value of the G13D mutant or that of the G12V or G12D mutant. Corresponds to Fig. 3B, but uses Ras-GTP Effector complex as the readout of signal strength.

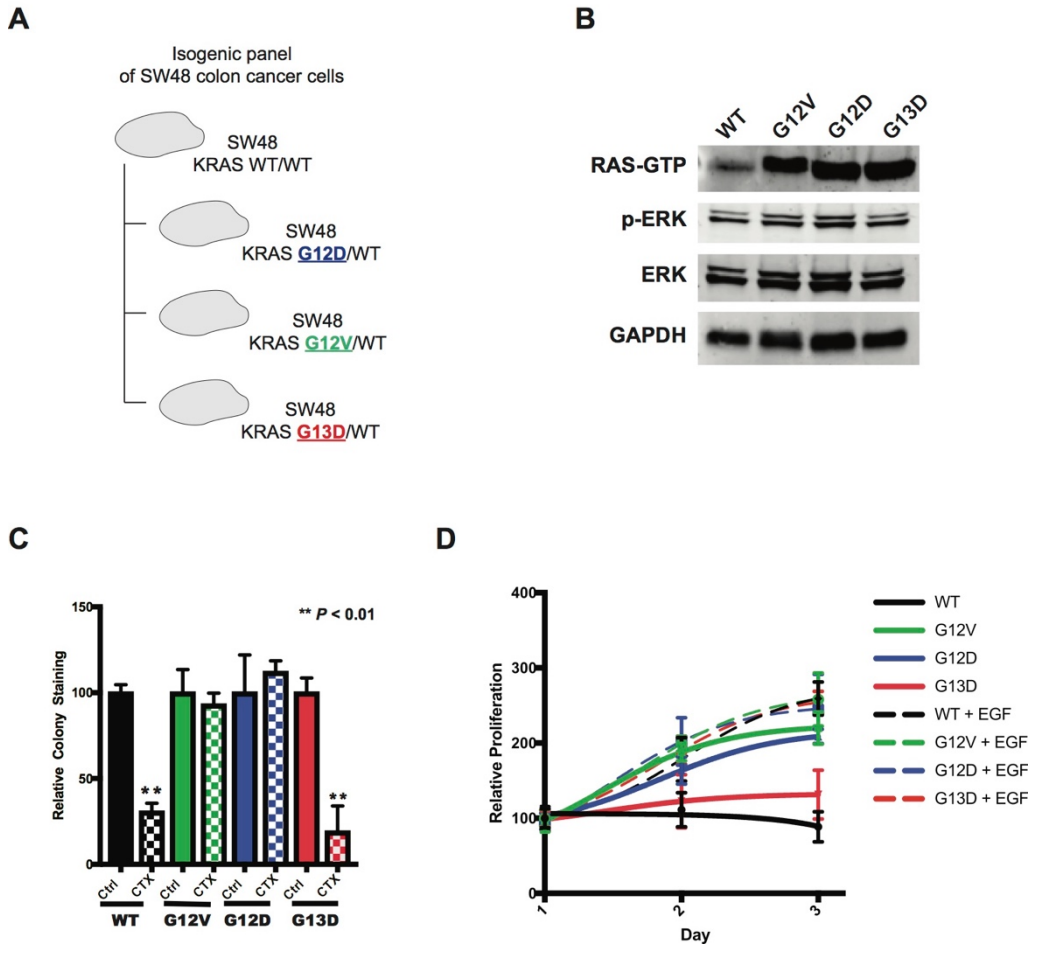

Fig. S4. Isogenic colon cancer cells display a KRAS mutant specific response to cetuximab. (**A**) A panel of isogenic cells derived from *KRAS WT* SW48 colon cancer cells to express one each of the three most common KRAS mutations in colon cancer (*KRAS G12D*, *KRAS G12V*, and *KRAS G13D*). (**B**) Immunoblots of isogenic cell lysates, including RasGTP pulled down with a Ras Binding Domain (RBD), demonstrate the constitutive activation of these mutants. Blots are representative of three independent experiments. (**C**) Quantification of the colony formation assay for each cell line in the isogenic panel without and with cetuximab (20μg/ml for 7 days)**.** Data are means ± SD of the three biological replicates within one colony formation experiment, and are representative of six independent experiments. (**D**) MTT assay proliferation time course for the isogenic panel grown in low serum media (1% FBS) and in low serum media with supplementary EGF (1% FBS + 20 ng/ml EGF) for the indicated time. Data are means ± SD of the seven biological replicates within one proliferation assay, and are representative of three independent experiments. Statistical significance was determined by one-way ANOVA followed by post-hoc Tukey's test for multiple comparison. $^{**}P<0.01$.

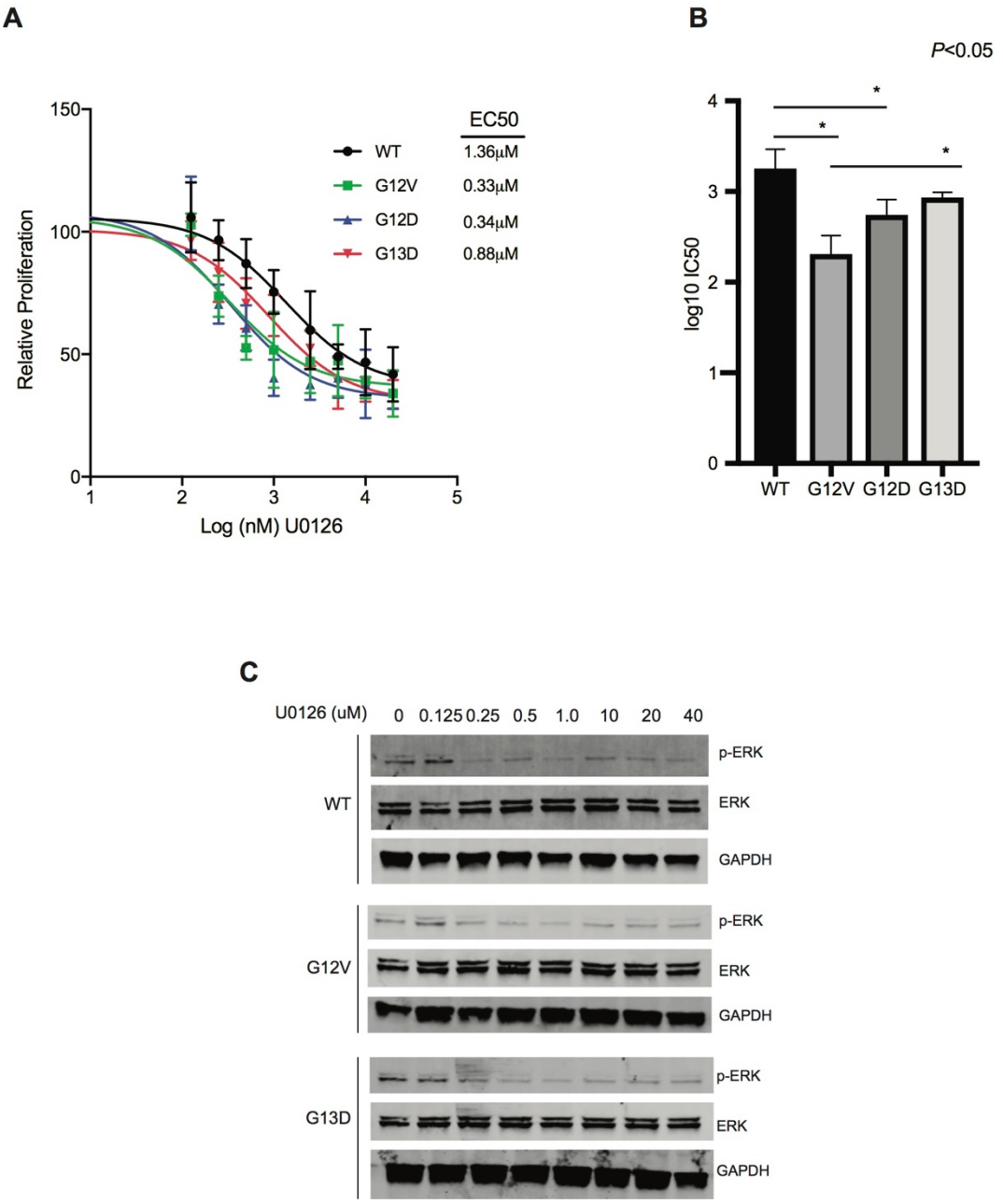

Fig. S5. Evaluation of the response of the isogenic panel to MEK inhibitor. (A) MTT proliferation assays to evaluate U0126 drug dose response for each cell line in the isogenic panel. Data are means ± SD for one dose response experiment, and are representative of three independent experiments. (B) Average IC50 values from three separate U0126 drug dose responses on isogenic SW48 cells. Statistical significance was determined by one-way ANOVA followed by post-hoc Tukey's test for multiple comparison. **P*<0.05. (**C**) Immunoblots of Ras pathway signaling for isogenic SW48 cells grown in different concentrations of U0126. Blots are representative of three independent experiments.

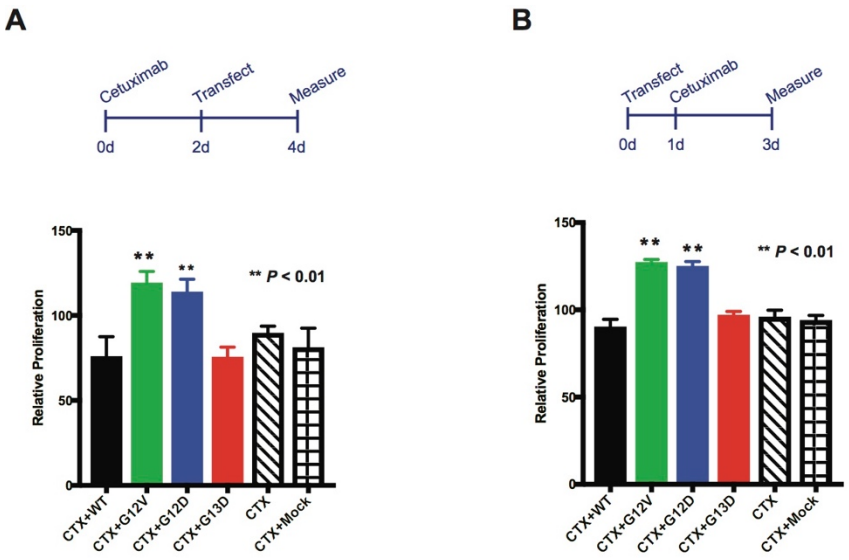

Fig. S6. Transfection based cetuximab sensitivity assay. (**A**) *KRAS WT* SW48 cells were treated with cetuximab (20 μg/ml) for two days, then transfected with KRAS G12V, G12D, G13D, or WT, and proliferation was assessed by MTT assays an additional two days later. (**B**) *KRAS WT* SW48 cells were transfected with KRAS G12V, G12D, G13D, or WT, allowed to recover for one day, treated with cetuximab (20 μg/ml), and proliferation was assessed by MTT assays an additional two days later. Data in both panels are means ± SD of the seven biological replicates within one proliferation assay, and are representative of three independent experiments. Statistical significance was determined by one-way ANOVA followed by post-hoc Tukey's test for multiple comparison. $^{**}P<0.01$.

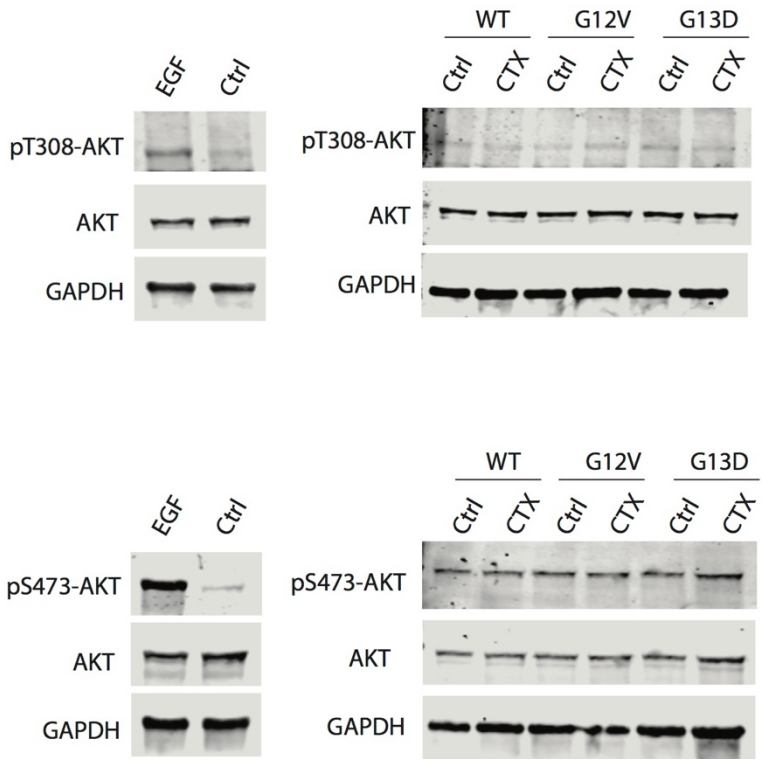

Fig. S7. Evaluation of AKT phosphorylation upon cetuximab treatment. AKT1 phosphorylation was assessed in starved, parental, *KRAS WT*, SW48 cells with and without 5 minutes of EGF stimulation (50 ng/ml for 5 minutes) for both Threonine 308 and Serine 473 (left). AKT phosphorylation was assessed in isogenic SW48 cells of the *WT*, *G12V*, and *G13D* genotypes with and without cetuximab treatment (20ug/ml for 48 hrs) (right). Blots are representative of two independent experiments.

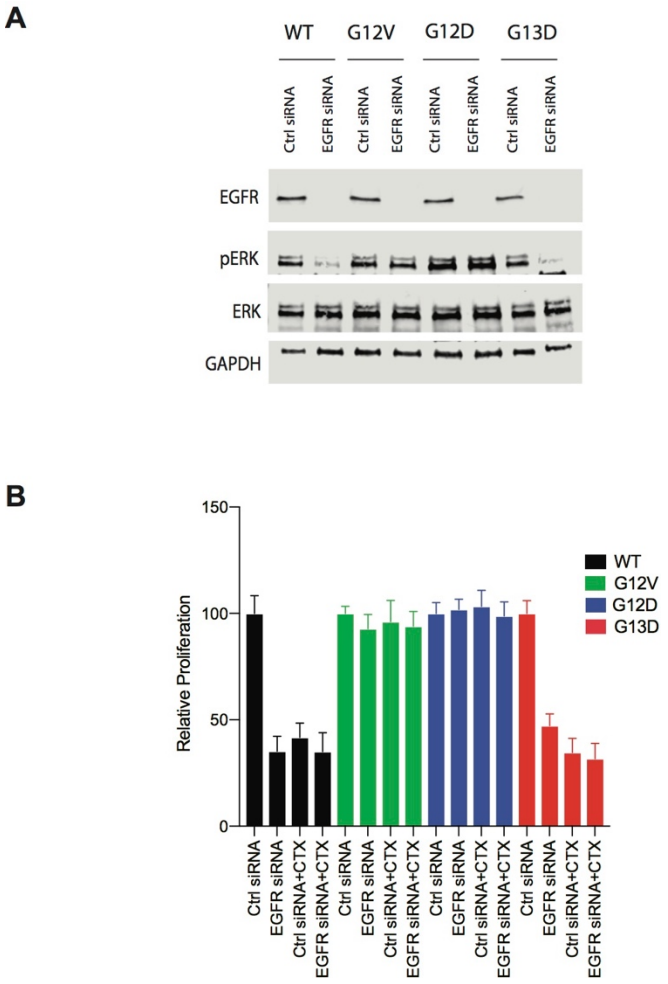

Fig. S8. Evaluation of EGFR knockdown for isogenic of SW48 cells. (**A**) Immunoblots of cell lysates from *WT*, *G12V*, *G12D*, and *G13D* isogenic SW48 cells after treatment with EGFR siRNA or with control siRNA. Blots are representative of three independent experiments. (**B**) MTT proliferation assays of isogenic SW48 cells of *WT*, *G12V*, *G12D*, and *G13D* genotypes after EGFR or control siRNA treatment, with or without additional cetuximab treatment (CTX; 20μg/ml) for 48 hrs. Data are means ± SD for one proliferation assay, and are representative of three independent experiments.

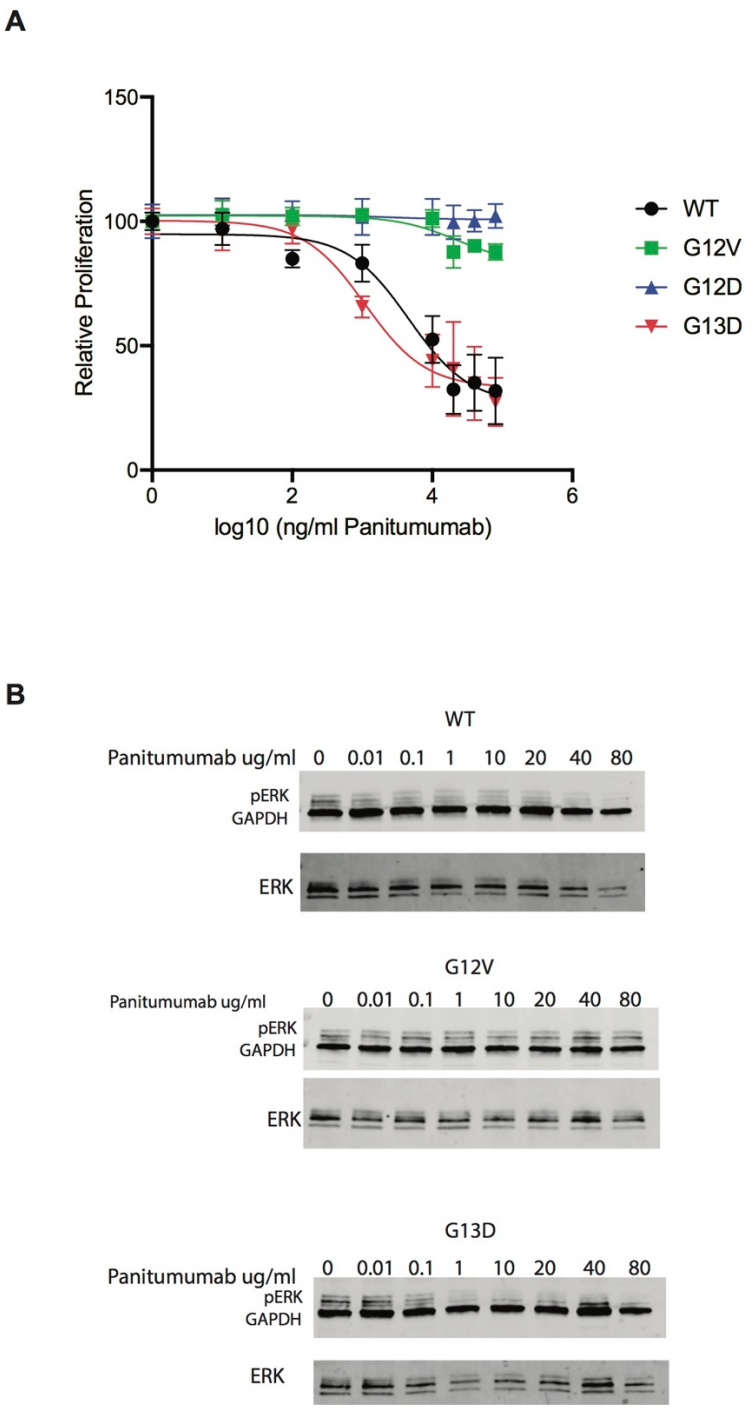

Fig. S9. Evaluation of panitumumab treatment of isogenic SW48 cells. (**A**) MTT proliferation assays to evaluate panitumumab drug dose response for each cell line in the isogenic panel. Data are means ± SD for one dose response experiment, and are representative of three independent experiments. (**B**) Immunoblots of Ras pathway signaling for isogenic SW48 cells grown in different concentrations of panitumumab. Blots are representative of three independent experiments.

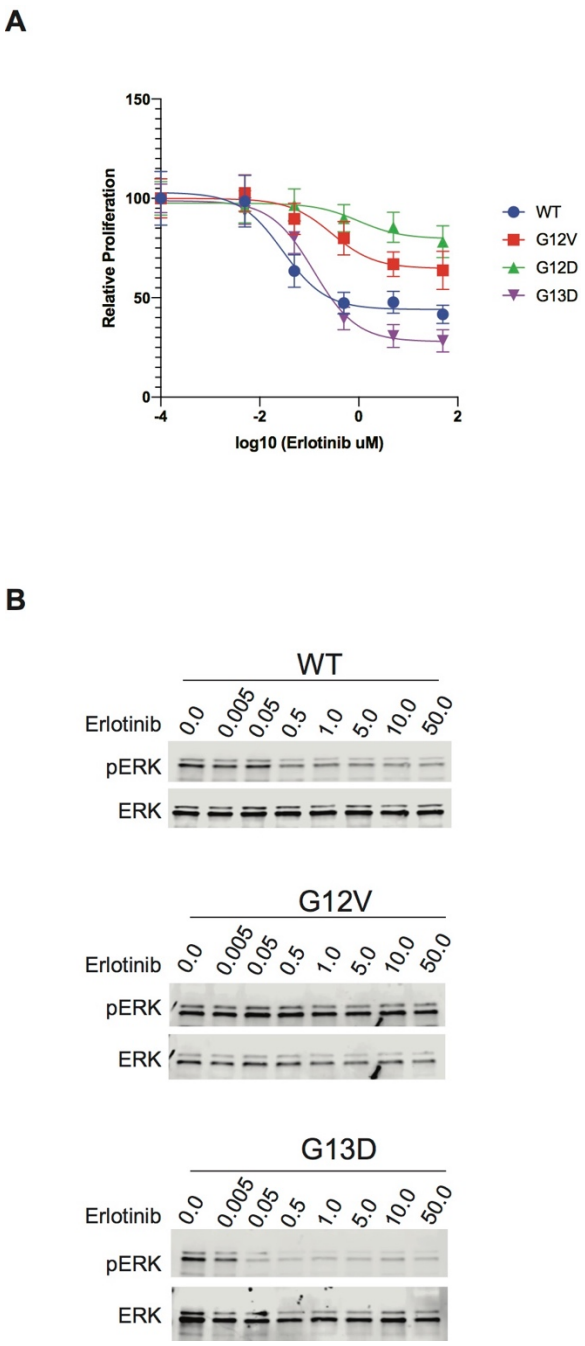

Fig. S10. Evaluation of erlotinib treatment of isogenic SW48 cells. (**A**) MTT proliferation assays to evaluate erlotinib drug dose response for each cell line in the isogenic panel. Data are means ± SD for one dose response experiment, and are representative of three independent experiments. (**B**) Immunoblots of Ras pathway signaling for isogenic SW48 cells grown in different concentrations of erlotinib. Blots are representative of three independent experiments.

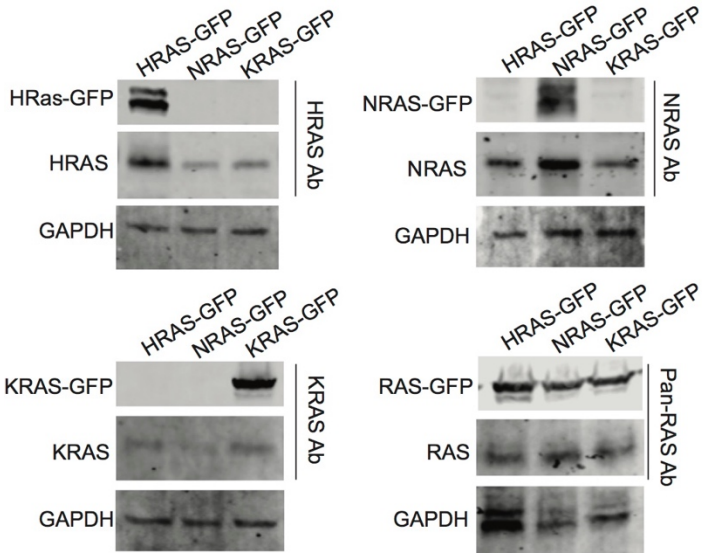

Fig. S11. Evaluation of Ras antibodies. 293T cells were transfected with HRAS-GFP, NRAS-GFP, or KRAS-GFP. Cell lysates from each were blotted with antibodies reported to be specific for HRAS, NRAS, KRAS, and pan (H/N/K) RAS. Blots are representative of three independent experiments.

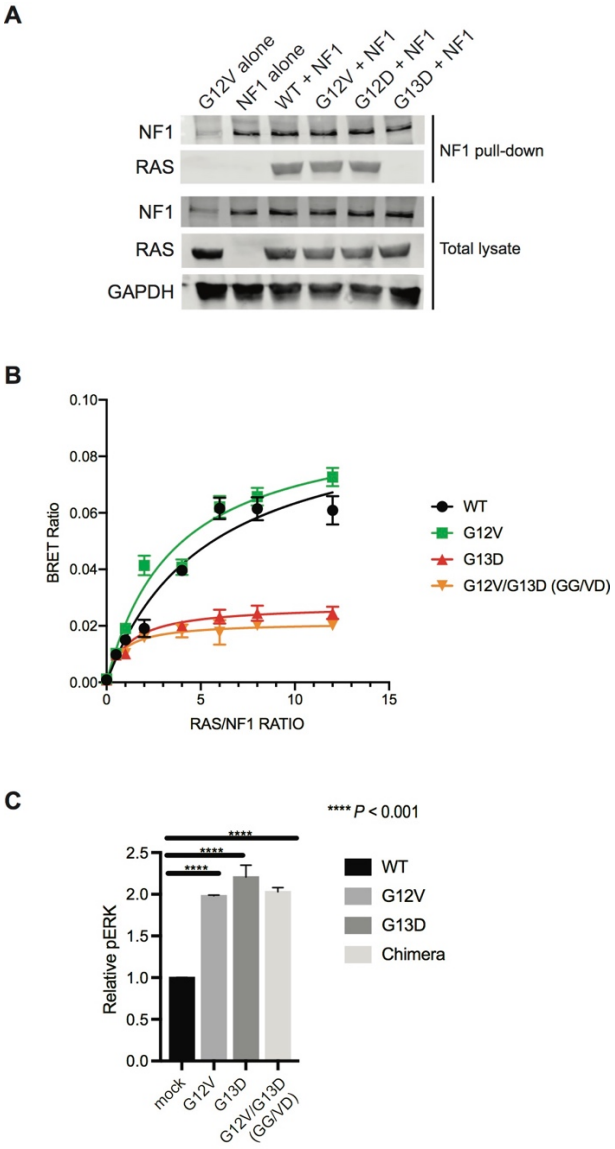

Fig. S12. Detection of impaired binding between KRAS G13D and NF1.
(**A**) Co-immunoprecipitation of Ras proteins with neurofibromin from mixtures of NF1-transfected 293T cell lysates with Ras transfected cell lysates. Blots are representative of three independent experiments. (**B**) Bioluminescence Resonance Energy Transfer (BRET) measurements of interactions between NF1-nanoLuc with EGFP tagged KRAS WT, KRAS G12V, KRAS G13D, and double mutant KRAS GG/VD (G12V/G13D) that were co-expressed in 293T cells. Data are means ± SD for one set of BRET assays, and are representative of three independent experiments. (**C**) Quantification of immunoblots of ERK phosphorylation, relative to total ERK, for parental, KRAS WT, SW48 cells transfected with KRAS G12V, KRAS G13D, or KRAS G12V/G13D (GG/VD) hybrid mutant or mock transfected. Data are means ± SD of three independent experiments. Statistical significance was determined by one-way ANOVA followed by post-hoc Tukey's test for multiple comparison. **** $P < 0.001$.

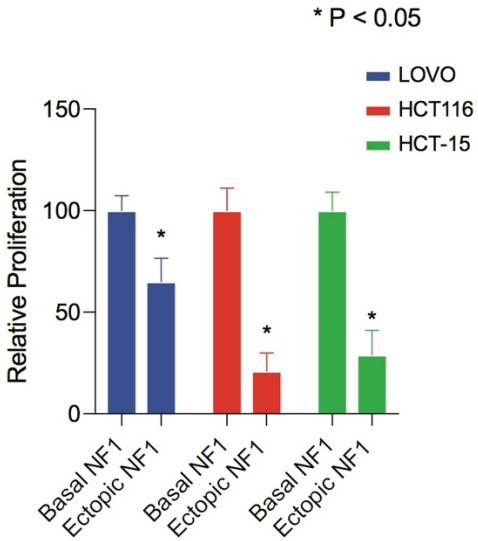

Fig. S13. Evaluation of KRAS G13D CRC cell lines that have been transduced with NF1. MTT proliferation assay of LoVo, HCT116, and HCT-15 cells (basal) compared with the same cells that have been lentivirally transduced to express ectopic NF1. Data are means ± SD for one proliferation assay, and are representative of three independent experiments. Statistical significance was determined by one-way ANOVA followed by post-hoc Tukey's test for multiple comparison. * $P < 0.05$.